COASTING BEAM LONGITUDINAL COHERENT INSTABILITIES

J.L. Laclare

ESRF, Grenoble, France

Abstract

Nowadays, the performance of most machine are limited by coherent instabilities. It is one of the most important collective effects which prevents the current from being increased above a certain threshold without the beam quality being spoiled. An intense cool beam (high intensity contained in a small phase space volume) is always unstable. A small density perturbation in the particle distribution, which can be due to either previous beam manipulations or even statistical noise (related to the point-like aspect of the particles), can grow exponentially by driving the entire beam into an unstable process. In phase space, the beam blows up, and becomes hot. With regards to the scope of the lecture, the physical mechanisms which will be considered throughout can be applied to any type of machine:

- linear accelerators,
- circular accelerators,
- storage rings

and beam:

- bunched beams
- continuous beams.

1. INTRODUCTION

In the first part of the lecture, we will limit ourselves to storage rings with a coasting beam which implies:

- Constant magnetic field
- no radio frequency applied.

These conditions are met in proton or heavy-ion cooler rings. They are also met in pulsed machines during injection or extraction of a debunched beam.

This regime does not exist on electron machines in which the RF is always on. With bunched beams, because of synchrotron motion, coherent instabilities manifest differently. However, the theoretical approach is essentially similar and easier to follow once the coasting beam case has been fully understood. The bunched beam case will be dealt with in the advanced course lecture.

The source of the instability can only be an electromagnetic field. With a very weak (very low intensity) beam, individual particles behave essentially like single particles. The external guiding field imposes the trajectories and has been designed so that these trajectories are stable.

With an intense beam, the large number of moving charges is responsible for the generation of an extra:

- "space-charge" field, or
- "self" electromagnetic field as shown in Fig. 1.

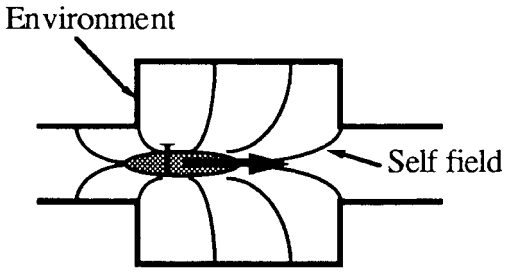

Fig. 1

If the intensity is large enough, this self field becomes sizeable in the sense that it can no longer be neglected when compared to the external guiding field. It can strongly influence the collective particle motion.

We will also limit ourselves to situations in which the external guiding field magnitude largely dominates. In other words, particle behaviour is still almost single particle behaviour. The self field acts as a perturbation.

As far as units are concerned, all formulae will be written in the International System units. Our formulae will make extensive use of the following standard quantities:

$$\begin{gathered} \varepsilon_0 = 8.854\ 10^{-12}\ \text{A s} \\ \mu_0 = 4\ \pi\ 10^{-7}\ \text{V s A}^{-1}\text{m}^{-1} \\ c = 2.998\ 10^{8}\ \text{m s}^{-1} \\ \varepsilon_0 \mu_0\ c^2 = 1 \\ e = 1.602\ 10^{-19}\ \text{A s} \end{gathered} \tag{1}$$

The self field follows Maxwell's equations.

We will do our best to avoid detailed calculations of electromagnetic fields and therefore to make explicit reference to their form. However, since these equations govern the fields and therefore the source of the instabilities, it is advisable to keep them in mind. Let E and B be the electric field and magnetic induction respectively. Then, $\vec{E}$ and $\vec{B}$ can be drawn from the potentials

$$\text{V and } \vec{A} \text{ solutions of : } \Delta V - \frac{1}{c^2}\frac{\partial^2 V}{\partial t^2} = -\frac{\rho}{\varepsilon_0}$$

where ρ is the particle charge density

$$\Delta\vec{A} - \frac{1}{c^2}\frac{\partial^2 \vec{A}}{\partial t^2} = -\mu_0 \vec{j} \tag{2}$$

where $\vec{j}$ is the particle current density by means of

$$\vec{E} = -\overrightarrow{\text{grad}\ V} - \frac{\partial}{\partial t}\vec{A} \text{ and } \vec{B} = \text{rot } \vec{A}$$

Obviously, boundary conditions which depend on the geometry and electromagnetic

properties of the environment (vacuum chamber, surrounding magnets, etc.) strongly influence the solution and therefore the perturbed motion of particles.

2 . SINGLE-PARTICLE MOTION

We will first ignore the self field and consider the unperturbed single particle motion. For a coasting beam, in the first order, the longitudinal motion is very simple.

$$\frac{d\vec{p}}{dt} = e\,[\,\vec{E} + \vec{v} \times \vec{B}\,] \tag{3}$$

For the longitudinal component

$$\frac{dp_{//}}{dt} = e\,[\,E_{//} + (\vec{v} \times \vec{B})_{//}\,] \tag{4}$$

there is no longitudinal field, no RF

$$E_{//} \text{ is nul and } (\vec{v} \times \vec{B})_{//} \text{ is a second order term} \tag{5}$$

Therefore,

$$\frac{dp_{//}}{dt} = 0 \quad p_{//} \text{ is a constant of the motion} \tag{6}$$

The revolution period T around the orbit length L is written:

$$T = \frac{2\pi}{\omega} = \frac{L}{\beta c} \tag{7}$$

It depends on the particle momentum and can be expanded in terms of momentum deviation.

Let us choose a reference (machine axis for instance)

$$p_{//0} = m_0 \gamma_0 \beta_0 c \tag{8}$$

Let us then expand:

$$\beta = \beta_0 \left(1 + \frac{1}{\gamma_0^2} \frac{p_{//} - p_{//0}}{p_{//0}} \right) \text{ and } L = L_0 \left(1 + \alpha \frac{p_{//} - p_{//0}}{p_{//0}} + .. \right) \tag{9}$$

$$L_0 = 2\pi R \text{ is the perimeter of the machine}$$
$$\alpha = \frac{p_{//}}{L} \frac{\partial L}{\partial p_{//}} \text{ momentum compaction} \tag{10}$$

$$\text{in smooth machines } \alpha \approx \frac{1}{Q_x^2} \text{ where } Q_x^2 \text{ is the horizontal betatron tune}$$

Second- and higher-order contributions to orbit lengthening (transverse peak amplitude

$\hat{x}$ and $\hat{z}$ dependence for instance) are neglected.

It is usual to write:

$$\frac{dT}{T} = \eta \frac{dp_{//}}{p_{//}} = - \frac{d\omega}{\omega} \quad \text{with } \eta = \alpha - \frac{1}{\gamma_0^2} = \frac{1}{\gamma_t^2} - \frac{1}{\gamma_0^2} \tag{11}$$

$$\gamma t = \frac{1}{\alpha^{1/2}} \text{ defines the transition energy}$$

$$E_t = m_0 \gamma_t \quad c^2 \tag{12}$$

Below transition: $E_0 < E_t$ and $\eta < 0$ particles with a positive momentum deviation circulate faster than the reference.

Above transition : $E_0 > E_t$ and $\eta > 0$ particles with a positive momentum deviation circulate slower than the reference.

When dealing with longitudinal (//) or transverse ($\perp$) instabilities the sign of η is essential. It indicates whether the slow particles at the tail, moving in the wake field, have a higher or lower energy than the fast particles at the front which create this wake field.

In order to describe trajectories two coordinates are necessary. Let $p_{//_0}$ and ω_0 in rad s^{-1} be the momentum and angular revolution frequency respectively for the reference. We define two coordinates attached to the reference particle frame.

$$\tau \quad \text{and} \quad \dot{\tau} = \frac{d\tau}{dt}$$

τ is expressed in s (seconds) and represents the time delay between the passing of the reference particle and the test particle at the same point around the circumference.
$\dot{\tau}$ is the time derivation of τ. The couple $(\tau, \dot{\tau})$ defines the coordinates of the test particle in the longitudinal bidimensional phase space.

With the definition of η as given above:

$$\dot{\tau} = \frac{dT}{T} = \eta \frac{dp_{//}}{p_{//}}$$

is a constant of the motion. Accordingly, the time delay: $\tau = \tau_0 + \dot{\tau}\ t$ is a linear function of time.

The differential equation of motion is:

$$\ddot{\tau} = \frac{\eta}{p_{//0}} \frac{dp_{//}}{dt} = \frac{\eta e}{p_{//0}} \left[\vec{E} + \vec{v} \times \vec{B}\right]_{//} (t,\theta) \qquad (13)$$

Until now the right hand side has been null. Later on it will take into account the self field as a perturbation.

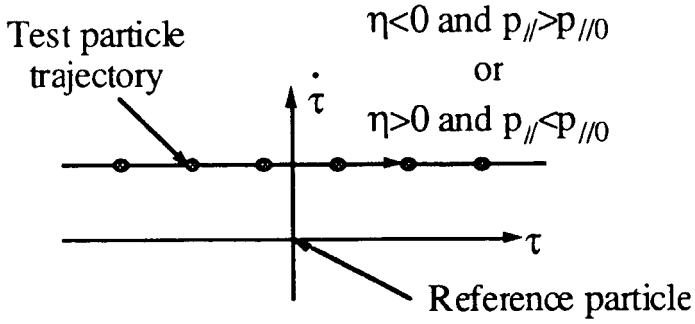

Fig. 2

3. LONGITUDINAL SIGNAL OF A SINGLE PARTICLE

With a view to expressing the self field, one has to solve Maxwell's equations. On the right hand side of Maxwell's equation, the expression of the beam current density $\vec{j}(t,\theta)$ and therefore of the current which will be noted $S_{//}(t,\theta)$ (in Ampere) is required.

Machine physicists are used to visualizing the beam current by looking with an oscilloscope at the signal drawn from longitudinal PU electrodes. We will assume a perfect longitudinal PU electrode with infinite bandwidth located at position θ around the ring. We will also assume that a single test particle rotates in the machine. At time $t = 0$ the fictive reference is at $\theta = 0$. The PU is located at position θ as shown in Fig. 3.

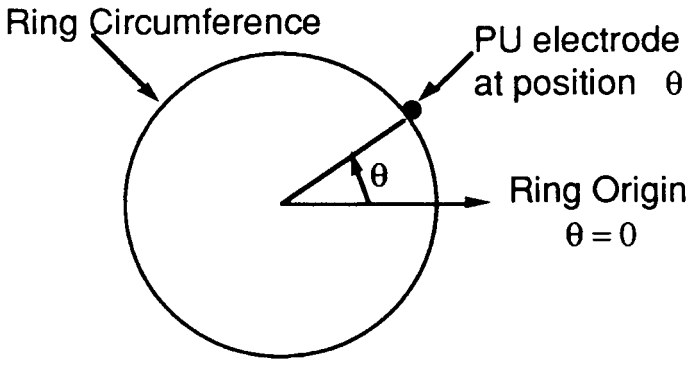

Fig. 3

The reference loops its turn with a period T_0 and passes at the PU location at times:

$$t_0^p = \frac{1}{\omega_0} (\theta + 2 p \pi) \qquad (14)$$

The test particle is delayed by τ_0 at time $t = 0$. It arrives at the PU at times:

$$t^p = t_0^p + \tau = \tau_0 + t_0^p \, (1 + \dot{\tau}) \tag{15}$$

The elementary signal is a series of periodical impulses delivered at each passage :

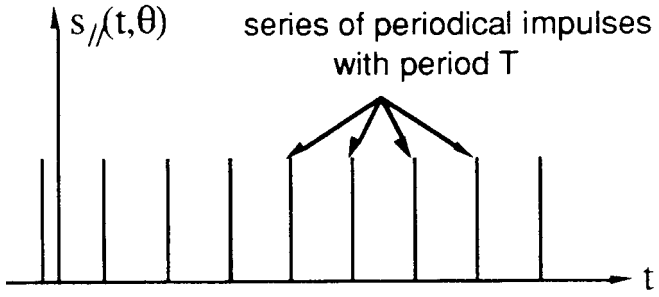

Fig. 4

The period T depends on the test particle momentum:

$$T = T_0 \, (1+\dot{\tau}) = T_0 \, (1+\eta \, \frac{p_{//} - p_{//0}}{p_{//0}} \tag{16}$$

The mathematical expression of the signal is:

$$s_{//} \, (t,\theta) = e \sum_{p = -\infty}^{p = +\infty} \delta[t - \tau - \frac{1}{\omega_0} \, (\theta + 2 \, p \, \pi) \tag{17}$$

where

$$\delta[.] \text{ is the Dirac function} \tag{18}$$

The series of periodical Dirac functions can be transformed into a series of exponential functions:

$$s_{//} \, (t,\theta) = \frac{e\omega_0}{2\pi} \sum_{p = -\infty}^{p = +\infty} \exp \, jp[\omega_0(t - \tau) - \theta] \qquad \text{where } j^2 = -1 \tag{19}$$

and

$$\tau = \tau_0 + \dot{\tau}t \tag{20}$$

Under this form, the signal can easily be Fourier analysed in the frequency domain.

$$s_{//}(\Omega,\theta) = \frac{1}{2\pi}\int_{t=-\infty}^{t=+\infty} s_{//}(t,\theta)\exp(-j\Omega t)\,dt$$

$$= \frac{e\omega_0}{2\pi}\sum_{p=-\infty}^{p=+\infty}\delta\{\Omega - p\omega_0(1-\dot{\tau})\}\exp -jp[\omega_0\tau_0 + \theta] \qquad (21)$$

The latter expression shows that when plugging the signal on a spectrum analyser, with Ω along the horizontal axis, we get a series of infinitely sharp lines at all harmonics $p\omega$ of the test particle revolution frequency: $\omega = \omega_0(1-\dot{\tau})$ with p running from $-\infty$ to $+\infty$

$$\Omega_p = p\omega = p\omega_0(1-\dot{\tau}) \qquad (22)$$

The spectral power amplitude is the same for all harmonics.

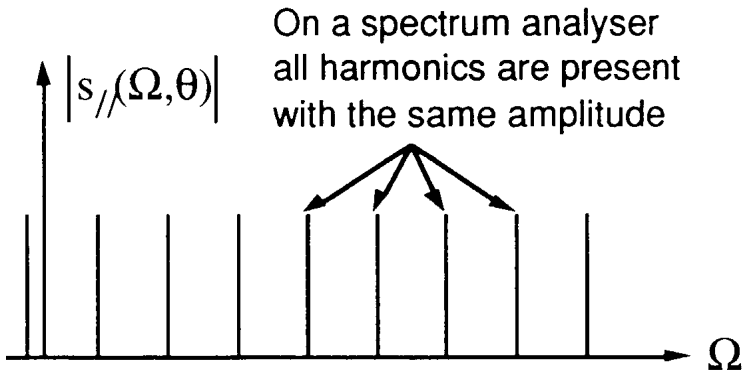

Fig. 5

If one considers a population of test particles with different momentum $p_{//}$ and therefore $\dot{\tau}$, then the width of the frequency band around harmonic p is proportional to p.

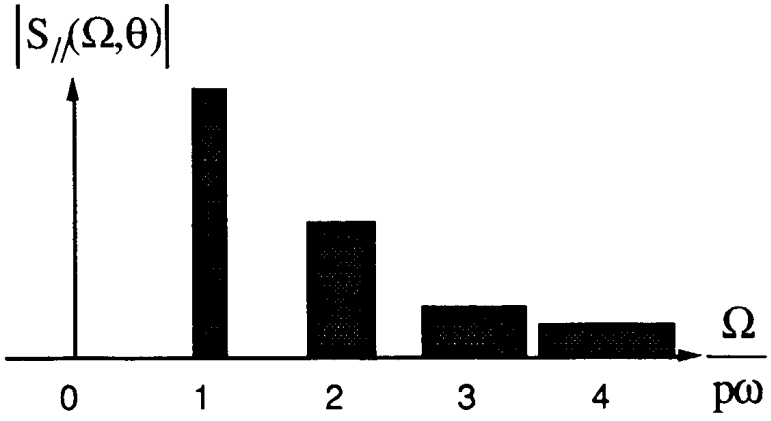

Fig. 6

In the above figure, the noise spectrum of a coasting beam with a uniform population of particles between two momenta

$$\pm \frac{\delta p_{//}}{p_{//0}} = \pm \frac{\hat{\dot{\tau}}}{|\eta|} \tag{23}$$

symmetric with respect to the reference particle momentum is sketched.

One can anticipate an overlap of the frequency bands for |p| values larger than or equal to p_{0v} with:

$$\frac{1}{2p_{0v}+1} = |\eta| \frac{\delta p_{//}}{p_{//0}} \tag{24}$$

These bands are called incoherent frequency bands.

The adjective incoherent is used to specify the fact that particles behave like independent particles, there beeing no coupling between them.

In accelerator physics, the electromagnetic noise picked up from the beam by means of a spectrum analyser is often called a Schottky scan. These longitudinal Schottky scans of a coasting beam make it possible to measure the momentum distribution within the beam.

4. DISTRIBUTION FUNCTION

In the previous section, we obtained the expression of the current or signal of a single particle. Maxwell's equations require the total beam current. This can be obtained by adding the individual signals of all the single particles constituting the beam.

To obtain a general mathematical expression, we introduce a distribution function: $\Psi(\tau,\dot{\tau},t)$ which represents the particle density in the bidimensional phase space and we write the signal of the entire beam:

$$S_{//}(t,\theta) = N\int_{\tau=0}^{\tau=T}\int_{\dot{\tau}=-\infty}^{\dot{\tau}=+\infty}\Psi(\tau,\dot{\tau},t)s_{//}(t,\theta)d\tau d\dot{\tau} \tag{25}$$

N is the total number of particles and therefore the following normalization is assumed:

$$1 = \int_{\tau=0}^{\tau=T}\int_{\dot{\tau}=-\infty}^{\dot{\tau}=+\infty}\Psi(\tau,\dot{\tau},t)d\tau d\dot{\tau} \tag{26}$$

Let us now introduce some basic notions and definitions concerning distributions.

A distribution is called a stationary distribution when the density does not change with time around any point of the phase space. There are as many incoming particles as departing particles around this point. We have seen that phase space trajectories are horizontal lines. Therefore, any function of $\dot{\tau}$ only would satisfy our requirement.

On the contrary, a stationary Ψ cannot depend on τ. As a matter of fact, a τ dependence would automatically move to other points. Accordingly, a stationary coasting beam can be represented by:

$$\Psi(\tau,\dot{\tau},t) = g_0(\dot{\tau}) \tag{27}$$

Such a function can represent the distribution of an unperturbed beam. It must be pointed out that the resulting signal is constant in the time domain.

$$S_{//}(t,\theta) = I \tag{28}$$

In the frequency domain there is a single line at zero frequency:

$$S_{//}(\Omega,\theta) = I\,\delta(\Omega) \tag{29}$$

The whole rich frequency spectrum of the individual particles composing the beam has disappeared. Such a dc current can only generate a dc electromagnetic field with essentially a transverse electric field and an azimuthal magnetic field.

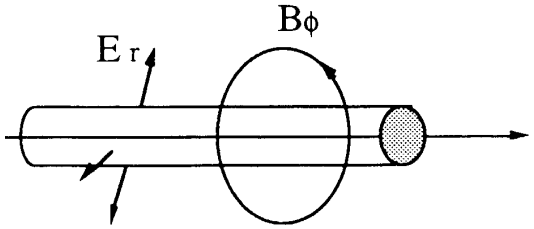

Fig. 7

The right hand side of the differential equation is null.

$$\ddot{\tau} = \frac{\eta}{p_{//0}}\frac{dp_{//}}{dt} = \frac{\eta e}{p_{//0}}\,[\vec{E} + \vec{v}\times\vec{B}]_{//}(t,\theta) = 0 \tag{30}$$

There is no force to drive an instability.

The conclusion is that a perfect coasting beam is always stable. In fact, a perfect coasting beam does not exist. A beam is a collection of point-like moving charges. On an average it can be represented by a stationary distribution. However, on top of it, some statistical noise is always present (Schottky scans).

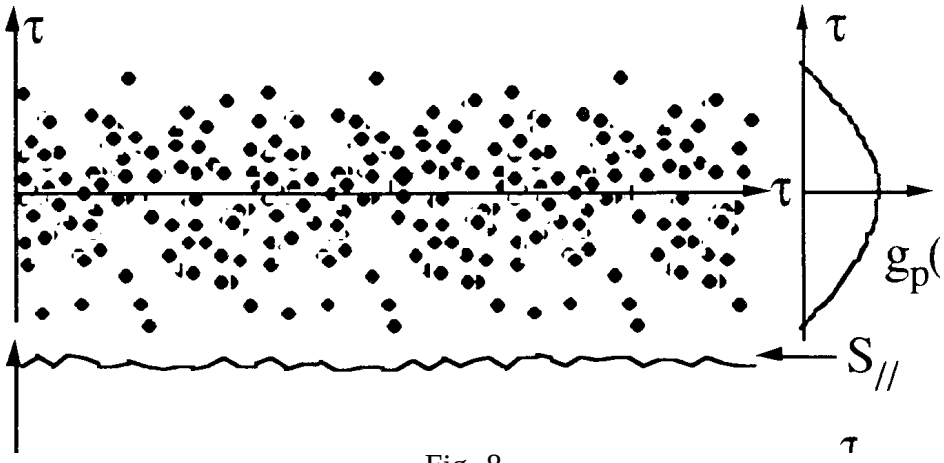

Fig. 8

When we used an integral over a distribution function (instead of a sum over individual particles) to draw the signal of the entire beam, we removed this noise. In addition, there are always distribution defects remaining as a memory of previous beam manipulations (injection kickers, remaining RF structure from a linac or a booster injector, etc...). Therefore, there are physical reasons for representing the beam by the sum of a stationary distribution plus a perturbation. Any density perturbation is automatically periodic in τ with a period T0. We will consider a single harmonic: harmonic p of the circumference. Accordingly, we assume a perturbation which consists of a prebunching of the beam with p wavelengths around the ring.

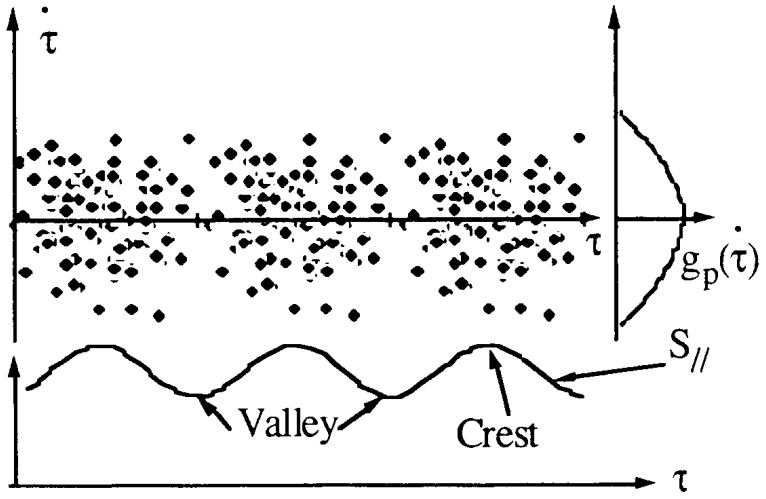

Fig. 9

This can be obtained with a term like:

$$g_p(\dot{\tau}) \exp jp\omega_0\tau \tag{31}$$

In addition, there is no reason to imagine that the perturbation will move exactly with the average particle frequency ω_0. We will assume a slight frequency shift: $\omega_{//pc}$
This can be obtained by multiplying the previous term by:

$$\exp j\omega_{//pc}t \tag{32}$$

Finally, we assume:

$$\Psi(\tau,\dot{\tau},t) = g_0(\dot{\tau}) + g_p(\dot{\tau}) \exp j(p\omega_0\tau + \omega_{//pc}t) \tag{33}$$

For reasons of normalization:

$$\int_{\dot{\tau}} g_0(\dot{\tau})\, d\dot{\tau} = \frac{1}{T_0} \tag{34}$$

$$\int_{\tau,\dot{\tau}} g_p(\dot{\tau}) \exp j(p\omega_0\tau + \omega_{//pc}t)\, d\tau\, d\dot{\tau} = 0 \tag{35}$$

The perturbation rearranges the particles but does not change the total number N.

Back to $\omega_{//pc}$, this frequency shift is a complex number.

$$\text{If } \mathrm{Im}(\omega_{//pc}) < 0 \tag{36}$$

The perturbation increases exponentially with time. The whole beam gets bunched on harmonic p. The growth rate for self bunching is given by:

$$\frac{1}{\tau_p} = -\,\mathrm{Im}(\omega_{//pc}) \tag{37}$$

On the contrary,

$$\text{If } \mathrm{Im}(\omega_{//pc}) > 0 \tag{38}$$

then, the perturbation is damped and disappears.

The signal induced by the above distribution is given by:

$$S_{//}(t,\theta) = I + S_{//p}(t,\theta)$$
$$\text{with} \tag{39}$$
$$S_{//p}(t,\theta) = IT_0 \exp j[(p\omega_0+\omega_{//pc})t-p\theta]\int_{\dot\tau} g_p(\dot\tau)d\dot\tau$$

and Fourier analysed:

$$S_{//}(\Omega,\theta) = I\,\delta(\Omega) + S_{//p}(\Omega,\theta)$$
$$\text{with} \tag{40}$$
$$S_{//p}(\Omega,\theta)=IT_0\exp(-jp\theta)\delta[\Omega-(p\omega_0+\omega_{//pc})]\int_{\dot\tau} g_p(\dot\tau)d\dot\tau$$

We find the dc component induced by the stationary distribution at zero frequency and in addition the frequency line induced by the perturbation at:

$$\Omega_c = p\omega_0+\omega_{//pc} \tag{41}$$

This frequency line is not an incoherent frequency line but on the contrary a coherent one in the sense that we had to arrange the particles by means of a distribution to obtain this line. We have assumed an initially coherent motion. The signal or current of the beam is a complex quantity. It will be associated with complex impedances (usual practice in classical electricity).

With a view to finding a solution for $\omega_{//pc}$, the next step is to write down the electromagnetic field induced by the beam.

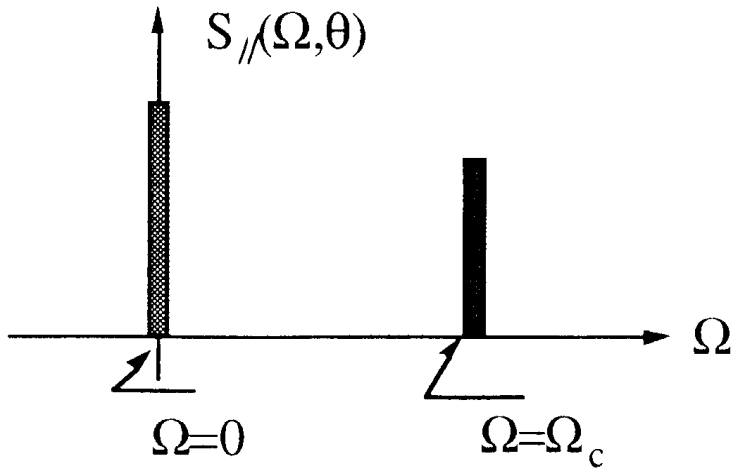

Stationary distribution Perturbation spectrum

Fig. 10

5. ELECTROMAGNETIC FIELD INDUCED BY THE BEAM

As already stated, the solution of Maxwell's equations depends on the boundary conditions imposed by the environment. It is obvious that:

– the detailed environment seen by the beam is different for different machines and changes around the circumference of a given ring.

– one cannot expect to analytically express exact solutions for the electromagnetic field with handy formulas.

In view of this, in this chapter we will consider the most simple type of environment and use the resulting electromagnetic field expression to introduce the notion of machine coupling impedance.

Let us consider a round beam of radius a travelling in a straight line along the axis of a circular pipe of radius b. For the time being, we will also assume a perfectly conducting pipe.

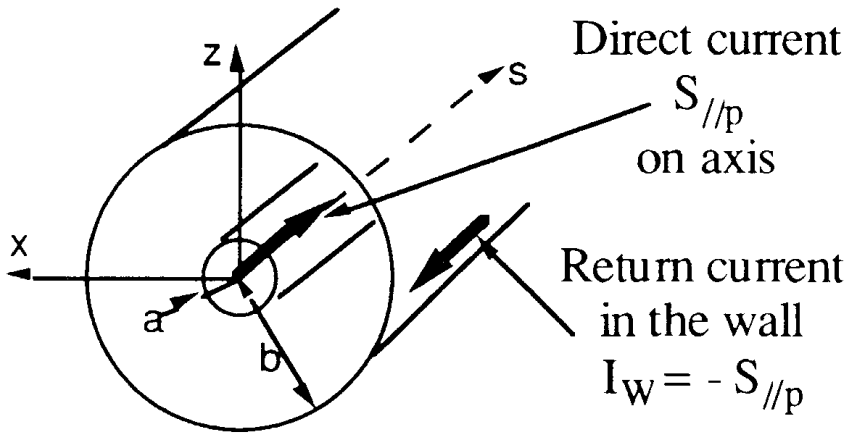

Fig. 11

With a perfectly conducting pipe, the solution of Maxwell's equations inside the pipe is independent of the environment outside the pipe. In particular the induced EM field is null outside the pipe and also in the wall thickness. It is completely stopped on the pipe inner surface by a return current $I_W = - S_{//p}$ uniformly distributed around the pipe, with the same amplitude as the direct signal but with the opposite sign.

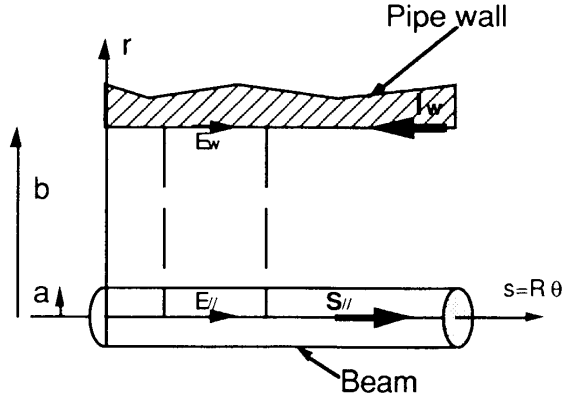

Fig. 12

Let :

$$E_{//}(t,\theta) = \widehat{E_{//}} \exp j(\Omega_c t - p\theta)$$

$$\Delta_{ab} = \frac{(K_1(z_a)I_0(z_b)+I_1(z_a)K_0(z_b)]}{I_0(z_b)} \qquad (42)$$

I_n and K_n being
the usual Bessel functions

Also let

$$z_r = \frac{\Omega_c r}{\beta\gamma c} \text{ for } 0 \le r \le a$$

Then

$$\widehat{E_{//}} = j\left(\frac{p^2}{R^2} - \frac{\Omega_c^2}{c^2}\right)\frac{\mu_0 \widehat{S_{//p}}}{\pi\Omega_c z_a}\left[\frac{1}{z_a} - \Delta_{ab} I_0(z_r)\right]$$

For this simple case of beam environment, the expression of the EM field is already complicated. In the longitudinal direction, the electric field is 90° out of phase with respect to the signal.

It is null on the crests and in the valleys of the line density when the signal is maximum, and maximum on the front and back slope when the signal is null.

Transversally, the field varies across the beam cross section:

$$I_0\left(\frac{\Omega_c\, r}{\beta\gamma c}\right) \text{ for } 0 \le r \le a \tag{43}$$

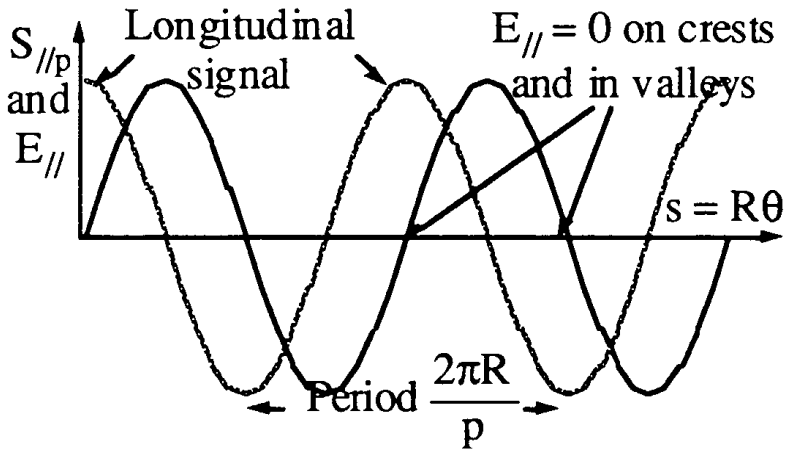

Fig. 13

This variation is small provided the argument of Bessel's function remains small at the beam edge and more generally across the pipe: r = b.

$$z_b = \frac{\Omega_c\, b}{\beta\gamma c} \ll 1$$
$$\text{where } \Omega_c = p\omega_0 + \omega_{//pc} \approx p\omega_0 = p\frac{\beta c}{R} \tag{44}$$

$$\text{For } z_b = 1 \; ; \; \gamma\frac{2\pi R}{p} = 2\pi b \tag{45}$$

The longitudinal wavelength with a relativistic correction γ in the direction of motion is equal to the pipe perimeter, or the frequency of the perturbation is equal to the pipe cut-off frequency.

$$\Omega_c = \gamma\beta\frac{c}{b} = \gamma\beta\omega_{\text{pipe cut-off}} \tag{46}$$

The EM field configuration is drastically changed around and above the cut-off frequency.

Let us evaluate orders of magnitude.

$$\text{Assume } b = 0.03 \text{ m}$$
$$\omega_{\text{pipe cut-off}} = \frac{c}{b} = 1.\ 10^{10} \text{ rad s}^{-1} \tag{47}$$
$$f_{\text{pipe cut-off}} = \frac{\omega_{\text{pipe cut-off}}}{2\pi} = 1.6 \text{ GHz}$$

$$z_b = \frac{\Omega_c}{\beta\gamma w_{\text{pipe cut-off}}} = 1$$
$$\text{implies} \qquad (48)$$
$$f_c(z_b=1) = \beta\gamma\, f_{\text{pipe cut-off}} = \beta\gamma\ 1.6\ \text{GHz}$$

The frequency around which tthis is occurs depends very much on machine energy.

Consider two examples:

$$\begin{gathered} 50\ \text{MeV/Amu}\ \beta=0.3\ \gamma=1.05 \\ f_c(z_b=1) = 0.5\ \text{GHz} \\ \text{and } z_b \ll 1 \text{ leads to } f_c \le 50\ \text{MHz} \\ 100\ \text{GeV/Amu}\ \beta=1\ \gamma=101 \\ f_c(z_b=1) = 160\ \text{GHz} \\ \text{and } z_b \ll 1 \text{ leads to } f_c \le 16\ \text{GHz} \end{gathered} \qquad (49)$$

In the following, we will assume that we stand well below these limits, in which case a good approximation for the electric field can be obtained by using the development of Bessel's functions for small values of the argument.

$$\widehat{E_{//}}(t,\theta) = -\frac{1}{2\pi R}\frac{Z_0\, g}{2j\beta_0\gamma_0^2}\frac{\Omega_c}{\omega_0}\widehat{S_{//p}}(t,\theta)$$
$$\text{where} \qquad (50)$$
$$Z_0 = \mu_0\, c = 377\ \Omega$$
$$g = 1 + 2\,\text{Log}\left(\frac{b}{a}\right)$$

Under all these assumptions, we have obtained the usual handy expression of the "longitudinal space charge electric field". The $\beta_0\gamma_0^2$ dependence shows that this field can severely affect very low energy particles.

6. NEGATIVE-MASS INSTABILITY

In this section, a qualitative treatment of the longitudinal instability induced by space charge forces is presented. Immediate conclusions can be drawn from the fact that the space-charge electric field is 90° out of phase with respect to the signal. Then, the sign of η

$$\frac{d\omega}{\omega_0} = -\,\eta\,\frac{dp}{p_{//0}} \text{ with } \eta = \frac{1}{\gamma_t^2} - \frac{1}{\gamma_0^2} \qquad (51)$$

defines whether the perturbation amplitude increases (instability) or decreases (stability).
Below transition energy ($\eta < 0$)

– acceleration on the front slope (**2** in Fig. 14) means increased momentum and therefore higher revolution frequency. Particles move ahead.

– deceleration on the back slope (**3**) implies that particles will move backwards.

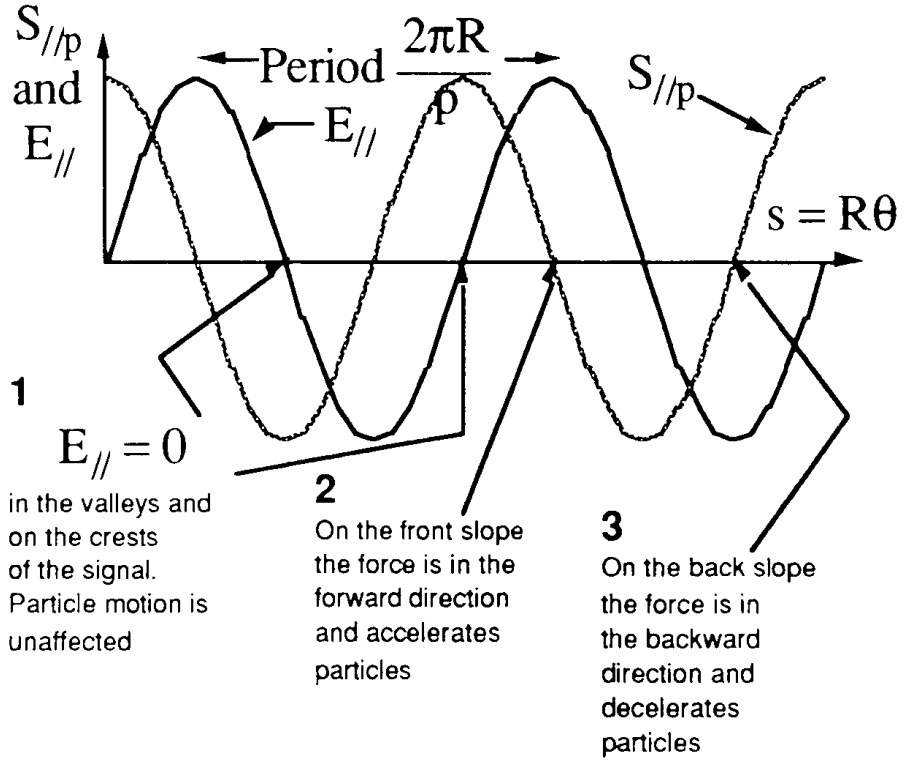

Fig. 14

Conclusion: Particles will move from the crests to fill the valleys and the initial perturbation will disappear.

It can be concluded that space charge has a stabilizing effect below transition energy. Obviously, the reverse applies above transition when $\eta > 0$. Above transition, space-charge fields make the coasting beam potentially unstable. This effect is commonly called negative-mass instability in view of the apparently strange fact that above transition, particles with higher energy go slower in the machine (longer trajectory even though their velocity is higher).

7. INTRODUCTION OF THE LONGITUDINAL COUPLING IMPEDANCE $Z_{//}(\omega)$

At this point, we could have started a quantitative treatment of the detailed motion of the perturbation. However, our pipe model of beam environment is very crude and our conclusions regarding stability would not be relevant to an actual machine. On the other hand, our mathematical possibilities are very limited. The analytical solution for the simple pipe model was complicated already. Extracting complete solutions of Maxwell's equations taking due account of an actual machine environment (all the changes of the geometry and electromagnetic properties of the vacuum chamber around the circumference) is definitely impossible. In order to remain as general as possible in our discussion about stability we shall introduce a new machine parameter: the longitudinal coupling impedance $Z_{//}(\omega)$

$Z_{//}(\omega)$ is in fact a parameter which can only be drawn once Maxwell's equations have

been completely solved. It gathers all the details of the electromagnetic coupling between the beam and the surroundings. By varying its form, we will be able to consider any type of beam self electromagnetic field.

To introduce this parameter, let us use the expression of the space charge field. This expression shows that the field is proportional to current.

$$\widehat{E_{//}}\,(t,\theta) = -\frac{1}{2\pi R}\left[\frac{Z_0\, g}{2j\beta_0\gamma_0^2}\frac{\Omega_c}{\omega_0}\right]\widehat{S_{//p}}\,(t,\theta) \tag{52}$$

It is written in a form identical to Ohm's law and the quantity between brackets must be expressed in Ω. This latter quantity will be called the longitudinal coupling impedance in general:

$$\widehat{E_{//}}\,(t,\theta) = -\frac{1}{2\pi R}Z_{//}(\omega)\,\widehat{S_{//}}\,(t,\theta) \tag{53}$$

and longitudinal space charge impedance in the present particular case with:

$$Z_{//SC}(\omega) = \frac{Z_0\, g}{2j\beta_0\gamma_0^2}\frac{\omega}{\omega_0} \tag{54}$$

At this stage, some generalization is necessary. Since both electric and magnetic forces act on the particles:

$$\ddot{\tau} = \frac{\eta}{p_{//0}}\frac{dp_{//}}{dt} = \frac{\eta e}{p_{//0}}\,[\vec{E} + \vec{v}\times\vec{B}]_{//}\,(t,\theta) \tag{55}$$

we include the magnetic field contribution in our definition and write:

$$[\vec{E} + \vec{v}\times\vec{B}]_{//}\,(t,\theta) = -\frac{1}{2\pi R}Z_{//}(\omega)\,S_{//}\,(t,\theta) \tag{56}$$

Up to now we have considered a pure perturbation at a single frequency. However, the most general beam signal spectrum (bunched beam for instance) is not limited to a single frequency but is spread over a wide frequency range.

Each individual frequency ω present in the Fourier transform of the signal contributes to the force and must be combined with the corresponding impedance at ω.

$$[\vec{E}+\vec{v}\times\vec{B}]_{//}(t,\theta) = \frac{-1}{2\pi R}\int_{\omega=-\infty}^{\omega=+\infty} Z_{//}(\omega)S_{//}(\omega,\theta)\exp j\omega t\, d\omega \tag{57}$$

in which the following definitions are assumed.

$$S_{//}(\omega,\theta) = \frac{1}{2\pi}\int_{t=-\infty}^{t=+\infty} S_{//}(t,\theta)\,\exp(-j\omega t)\,dt$$

and reciprocally (58)

$$S_{//}(t,\theta) = \int_{\omega=-\infty}^{\omega=+\infty} S_{//}(\omega,\theta)\,\exp\, j\omega t\, d\omega$$

With a view to obtaining an expression of $Z_{//}(\omega)$ in terms of physical quantities, let us apply the previous relation to a Dirac charge e rotating at frequency ω_0 in the machine.

$$S_{//}(t,\theta) = \sum_p e\delta(t-\frac{\theta+2k\pi}{\omega_0})$$

$$S_{//}(\omega,\theta) = \frac{e\omega_0}{2\pi}\sum_p \exp(-jp\theta)\,\delta(\omega-p\omega_0) \quad (59)$$

$$-2\pi R[\vec{E}+\vec{v}\times\vec{B}]_{//}(t,\theta) = \frac{e\omega_0}{2\pi}\sum_p Z_{//}(p\omega_0)\exp(jp(\omega_0 t-\theta))$$

We now follow the field particle while remaining τ behind it by taking $\theta=\omega_0(t-\tau)$ and obtain

$$-\frac{2\pi R}{e}[\vec{E}+\vec{v}\times\vec{B}]_{//}(\tau) = G(\tau) = \frac{\omega_0}{2\pi}\sum_p Z_{//}(p\omega_0)\exp(jp\omega_0\tau) \quad (60)$$

The voltage per unit charge $G(\tau)$ expressed in volts per Coulomb is usually called the Green function. It is expanded into a series over all harmonics of the revolution frequency.

If the impedance is smooth enough or the machine long enough so that the wake field is null after one revolution, the series can be approximated by an integral.

$$G(\tau) = \frac{1}{2\pi}\int_{-\infty}^{+\infty} Z_{//}(\omega)\,\exp(j\omega\tau)\,d\omega \quad (61)$$

This last expression can be inverted to obtain

$$Z_{//}(\omega) = \int_{-\infty}^{+\infty} G(\tau)\, \exp(-j\omega\tau)\, d\tau \qquad (62)$$

In other words, $Z_{//}(\omega)$ is the Fourier transform of $2\pi G(\tau)$.

Ideally, this relation can be used in numerical codes to calculate the function $Z_{//}(\omega)$. A short bunch of particles is sent on axis through a structure. Maxwell's equations are solved step by step at predetermined mesh points. This allows the Green function and afterwards its Fourier transform to be obtained numerically.

8. LONGITUDINAL COUPLING IMPEDANCE $\boxed{Z_{//}(\omega)}$ OF AN ACCELERATOR RING

Designers are confronted with the problem that they have to include in their machine all sorts of bellows, flanges, cross section changes, PU electrodes, RF gaps, kickers, septum magnets, etc., which influence the impedance. During the last two decades, progress has been made towards estimating impedances better. Numerical codes and experimental tools have been developed. However, RF properties are difficult to predict or measure and we are still far from the situation where we could predict the curve $Z_{//}(\omega)$ accurately enough before commissioning a machine. We have also learnt a lot from existing machines. Most of them suffering from instabilities despite many attempts to measure and lower their impedance.

As already stated, the impedance is a complex function of frequency. A priori, it has an imaginary part and a real part. The space charge impedance from a perfectly conducting round pipe was an example of a purely imaginary impedance. Basically, in the broad sense, a ring impedance can be inductive, or capacitive or resistive. Our equations are written in such a form that we have to consider the complete frequency axis (positive and negative ω). In addition, for reasons which will be understood later in the course of this lecture, the quantity of interest is not directly

$$Z_{//}(\omega) \text{ but } \frac{Z_{//}(\omega)}{\omega} \text{ or } \frac{Z_{//}(\omega)}{p} \text{ with } p = \frac{\omega}{\omega_0} \qquad (63)$$

Accelerator physicists are used to plotting

$$\mathrm{Im}\left(\frac{Z_{//}(\omega)}{\omega}\right) \quad \text{and} \quad \mathrm{Re}\left(\frac{Z_{//}(\omega)}{\omega}\right) \qquad (64)$$

with ω along the horizontal axis.

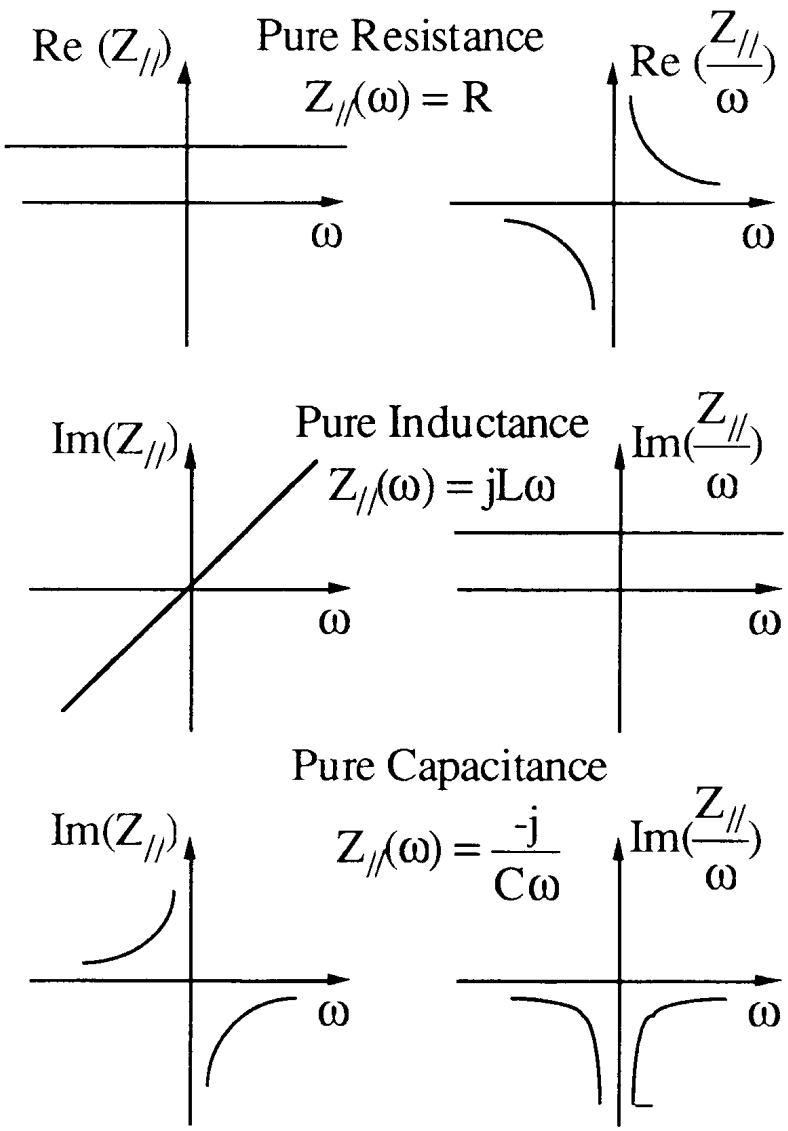

Fig. 15

In a standard machine, out of the four major components of the impedance, the first one is the space charge component already introduced.

$$\frac{Z_{//SC}(\omega)}{p} = -j\frac{Z_0\, g}{2\beta_0\gamma_0^2} \text{ where p stands for } \frac{\omega}{\omega_0} \tag{65}$$

It corresponds to a pure negative inductance (imaginary part only) very large for low energies. For instance:

$$\begin{aligned} &50 \text{ MeV/Amu } \beta_0=0.3\ \gamma_0=1.05\ g\cong 2.4\ \frac{Z_{//SC}}{p} = -j1.4\ k\Omega \\ &10 \text{ GeV/Amu } \beta_0=1\ \gamma_0=11.7\ g\cong 2.4\ \frac{Z_{//SC}}{p} = -j3.3\ \Omega \end{aligned} \tag{66}$$

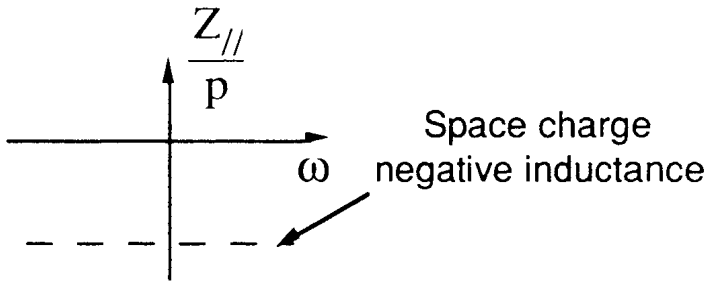

Fig. 16

The resistive wall impedance is the second major component.

Previously, the pipe was assumed to have a perfectly conducting wall (conductivity $\sigma = \infty$) and no resistance was opposed to the return wall current I_w. For finite σ, I_w flows in a strip of length $2\pi R$, width $2\pi b$, thickness δ : the skin depth at frequency ω. On top of the space-charge field, the beam sees a uniform longitudinal electric field set up by I_w. $\delta 0$ being the skin depth at frequency $\omega 0$. We will write:

$$\delta^2 = \delta_0^2 \frac{\omega_0}{\omega} \text{ with } \delta_0^2 = \frac{2}{\mu\sigma\omega_0} \tag{67}$$

and consider two regimes.

At very low frequency, the skin depth δ is larger than the wall thickness δw (thin wall). The impedance seen by I_w is the pipe resistance

$$Z_{//RW} = \frac{1}{\sigma}\frac{2\pi R}{2\pi b\delta_W} \quad \text{or} \quad \frac{Z_{//RW}}{p} = \frac{R}{\sigma b\delta_W}\frac{1}{p} \tag{68}$$

The impedance seen by the beam is exactly the same.

At high frequencies, the wall is thicker than the skin depth. It can be shown that the previous formula must be amended by replacing δw by δ and multiplying by (1+j) (an imaginary term appears).

$$\frac{Z_{//RW}}{p} = (1+j)\frac{R}{\sigma b\delta}\frac{\omega_0}{\omega} = (1+j)\frac{Z_0\beta_0\delta_0}{2b}\frac{1}{\sqrt{p}} \tag{69}$$

The transition between the two expressions occurs when $\delta = \delta w$.

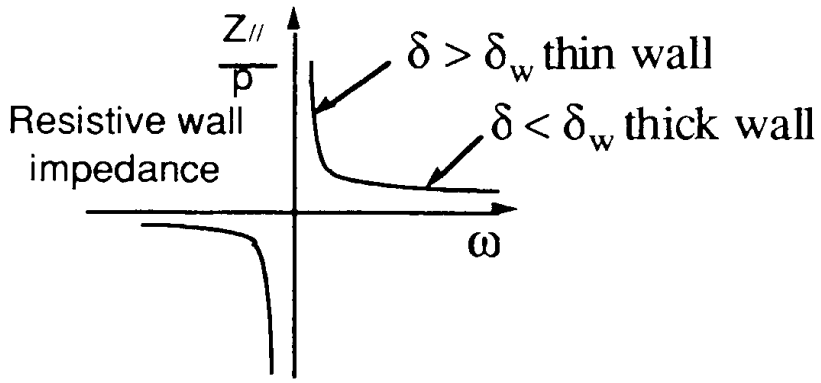

Fig. 17

The energy lost in the wall is drawn from the beam which is decelerated. As far as instabilities are concerned, the resistive wall impedance is not the source of problems in the longitudinal direction. It essentially affects the transverse motion.

The two last major components correspond to resonating objects. Let us start by some general definitions and remarks concerning resonators. The impedance of a resonator is often written:

$$Z_{//} = \frac{R_S}{1 + jQ(\frac{\omega}{\omega_r} - \frac{\omega_r}{\omega})} \tag{70}$$

R_S is the shunt impedance in Ω; Q the quality factor ; ω_r the resonant frequency

When the resonator is driven at very low frequency,

$$\omega = p\omega_0 \ll \omega_r \qquad \frac{Z_{//}}{p} = j\,\frac{R_S\omega_0}{Q\omega_r} \tag{71}$$

it behaves like a pure inductance. At resonance, it is a pure resistance.

$$\omega = p\omega_0 = \omega_r \qquad \frac{Z_{//}}{p} = R_S\frac{\omega_0}{\omega_r} \tag{72}$$

At high frequencies,

$$\omega = p\omega_0 \gg \omega_r \qquad \frac{Z_{//}}{p} = R_S\frac{\omega_0\omega_r}{jQ\omega^2} \tag{73}$$

it behaves like a pure capacitance.

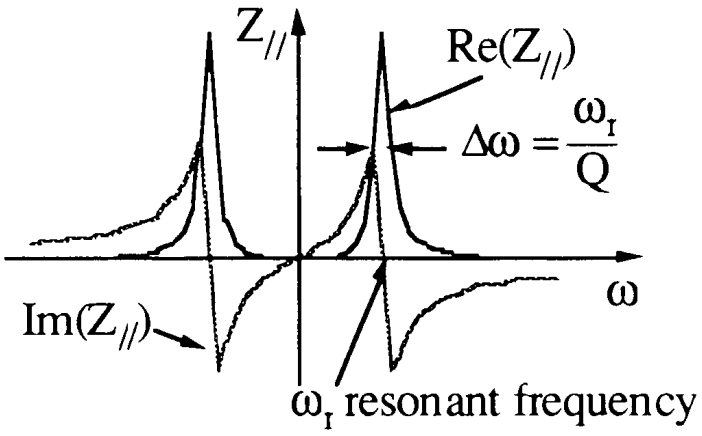

Fig. 18

As shown in Fig. 18, the real part is maximum (R_S) at the resonant frequency. The resonator bandwidth $\Delta\omega$ full width, half height is given by:

$$\Delta\omega = \frac{\omega_r}{Q} .$$

It can be shown that the time Δt during which a resonator of bandwidth $\Delta\omega$ memorizes the energy left by a Dirac excitation is given by:

$$\Delta\omega\Delta t = \frac{\omega_r}{Q}\Delta t \approx 1 \qquad (74)$$

(uncertainty principle).

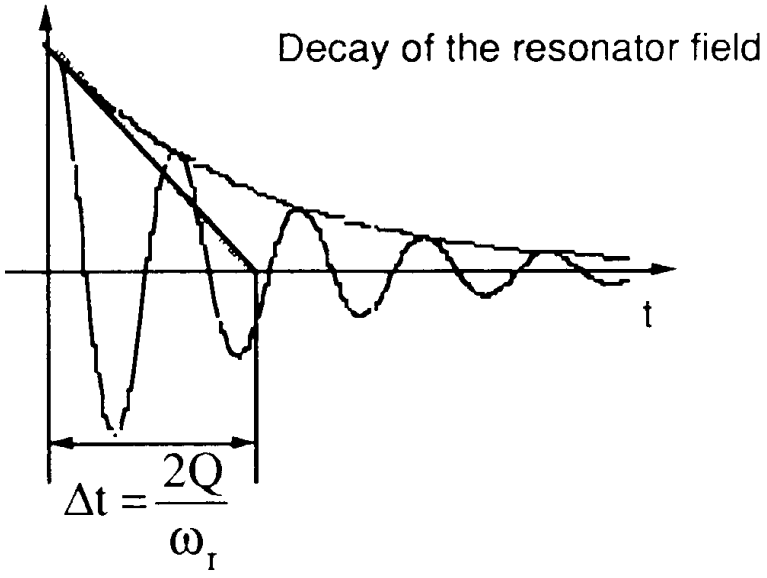

Fig. 19

The immediate consequence is that the response or wake field of a narrow-band resonator

(high Q and small $\Delta\omega$) lasts for a long time. Particles well separated in time are coupled by such a resonant object. The RF cavities are the most current sources of narrow-band resonators. They are tuned to resonate at the fundamental frequency $h\omega_0$. However, resonant higher-order longitudinal (and also transverse) modes with high Q are always present. The representation of a narrow-band resonator in the impedance diagram with $\frac{Z_{//}}{p}$ along the vertical axis is sketched below.

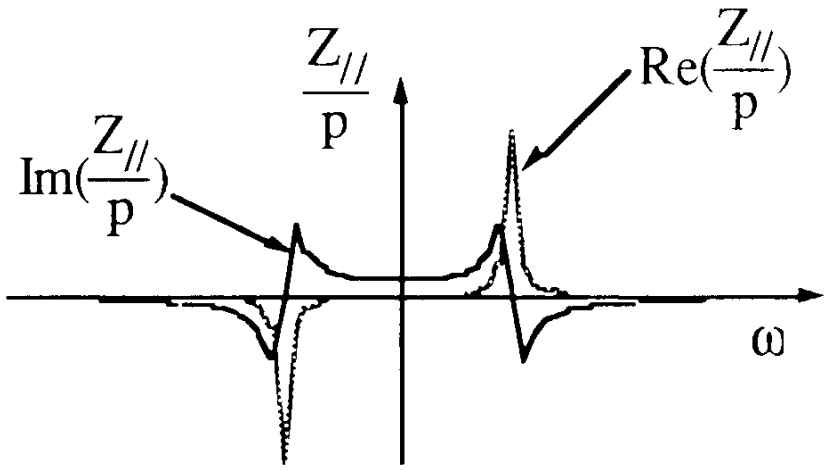

Fig. 20

Narrow band resonators constitute the third type of impedance usually met in an accelerator ring. The last component of the impedance corresponds to the numerous changes of cross sections, bellows, flanges, etc. It is obvious that these structures can trap some magnetic field and therefore behave like an inductance at low frequencies. This has been measured on existing machines.

We also learnt that when no special care is taken, the vacuum chamber is essentially resistive at frequencies around the pipe cut-off frequency. This is due to the fact that the path followed by the return current is very complicated and the resistance high when the vacuum chamber wall is not smooth or correctly shielded along the longitudinal axis. It has also been observed that the resistive part drops at frequencies higher than the cut-off frequency.

The object is to represent the above observations with the simplest impedance model. In this respect, a broad band resonator with a resonant frequency around the vacuum pipe cut-off frequency:

$$\omega_{rBB} \approx \omega_{cut\text{-}off} = \frac{c}{b} \tag{75}$$

can give an overall satisfactory result. To a certain extent, most experimental results drawn from existing rings have been correctly fitted by assuming the existence of such a component with $Q \approx 1$ (as sketched below) and a shunt impedance Rs adjusted to obtain the good value of the low frequency inductance.

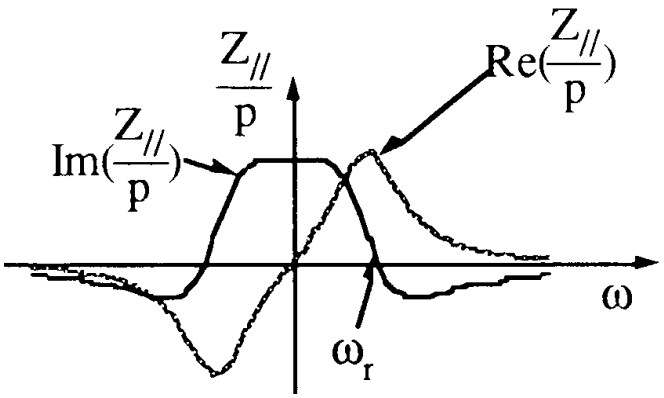

Fig. 21

Concerning orders of magnitudes, the full range

$$0.2\ \Omega \le \left|\frac{Z_{//}}{p}\right|_{max} = R_S \frac{\omega_0}{\omega_r} \le 50\ \Omega \tag{76}$$

has been found. The lowest values are obtained with modern machines. At present, a considerable effort is being put into designing a very smooth chamber. Unavoidable changes of cross section are systematically shielded and are no longer seen by the beam.

For such low-Q objects, the impedance curve varies slowly with frequency and the resonator bandwidth $\Delta\omega$ is large. Therefore, the wake field decays rapidly. It is a local interaction which can only couple particles close to each other along the longitudinal axis.

This handy broad band-model can only be used as a crude representation of reality. It will constitute the last component of our inventory of contributions to a ring impedance.

9. VLASOV'S EQUATION AND DISPERSION RELATION

At this point, all necessary ingredients to start the most general discussion on beam stability have been gathered.

– distribution function: $\Psi(\tau,\dot\tau,t) = g_0(\dot\tau) + g_p(\dot\tau)\ \exp\ j(p\omega_0\tau + \omega_{//pc}t)$ (77)

– perturbation signal: $S_{//_p}\ (t,\theta) = IT_0 \exp\ j[(p\omega_0+\omega_{//pc})t - p\theta] \int_{\dot\tau} g_p(\dot\tau)d\dot\tau$ (78)

– the general impedance of a ring $Z_{//}$,

– the general expression of the EM field generated by a signal in a ring with impedance $Z_{//}$

$$[\vec{E}+\vec{v}\times\vec{B}]_{//}(t,\theta) = \frac{-1}{2\pi R}\int_{\omega=-\infty}^{\omega=+\infty} Z_{//}\ (\omega)\ S_{//}\ (\omega,\theta)\exp\ j\omega t\ d\omega \tag{79}$$

$$[\vec{E}+\vec{v}\times\vec{B}]_{//}(t,\theta) = -\frac{1}{2\pi R} Z_{//}(\Omega_c)\, S_{//}(t,\theta) \tag{80}$$

in the present case.

$$= -\frac{I}{\beta_0 c} Z_{//}(\Omega_c)\exp j[\Omega_c t - p\theta]\int_{\dot{\tau}} g_p(\dot{\tau})d\dot{\tau} \tag{81}$$

where Ω_c stands for $p\omega_0+\omega_{//pc}$

when the expression of the perturbation signal is used.

– The EM force acts back on the particles,

$$\ddot{\tau} = \frac{\eta}{p_{//0}}\frac{dp_{//}}{dt} = \frac{\eta e}{p_{//0}}\,[\vec{E} + \vec{v}\times\vec{B}]_{//}(t,\theta) \tag{82}$$

in which $\theta = \omega_0(t-\tau)$ in order to follow the particle along its trajectory.

$$\ddot{\tau} = \frac{-\eta e I Z_{//}(\Omega_c)}{m_0\gamma_0 c^2\beta_0^2}\exp j[p\omega_0 t+\omega_{//pc}t]\int_{\dot{\tau}} g_p(\dot{\tau})d\dot{\tau} \tag{83}$$

The goal is to find out the solution

$$\Omega_c \text{ or } \omega_{//pc} \tag{84}$$

and to discuss beam stability via the imaginary part. The evolution of the distribution is governed by the collision-free Boltzmann equation:

$$\frac{\partial\Psi}{\partial t} + \mathrm{div}(\Psi\vec{v}) = 0 \tag{85}$$

This equation is similar to the one commonly used in electromagnetism for the charge density

$$\frac{\partial\rho}{\partial t} + \mathrm{div}\vec{j} = 0 \text{ with } \vec{j} = \rho\vec{v} \tag{86}$$

In our particular case:

$$\vec{v} = \begin{pmatrix}\overrightarrow{d\tau}\\ dt\end{pmatrix}\begin{pmatrix}\\ d\dot{\tau}\\ dt\end{pmatrix} \tag{87}$$

The equation can be developed $\frac{\partial\Psi}{\partial t} + \vec{v}\,\overrightarrow{\mathrm{grad}\Psi} + \Psi\,\mathrm{div}\,\vec{v} = 0$ (88)

and then simplified, since $\mathrm{div}\,\vec{v} = 0$ when canonical variables like $\tau,\dot{\tau}$ are used.

$$\frac{\partial \Psi}{\partial t} + \vec{v}\,\overrightarrow{\mathrm{grad}\Psi} = 0$$
$$\frac{\partial \Psi}{\partial t} + \frac{\partial \Psi}{\partial \tau}\dot{\tau} + \frac{\partial \Psi}{\partial \dot{\tau}}\ddot{\tau} = \frac{d\Psi}{dt} = 0 \qquad (89)$$

In this form, it is called Vlasov's equation.

We now apply Vlasov's equation to the assumed distribution :

$$\Psi(\tau,\dot{\tau},t) = g_0(\dot{\tau}) + g_p(\dot{\tau})\,\exp\, j(p\omega_0\tau + \omega_{//pc}t) \qquad (90)$$

and get:

$$\frac{\partial \psi}{\partial t} = j\omega_{//pc}\, g_p(\dot{\tau})\,\exp\, j(p\omega_0\tau + \omega_{//pc}t)$$
$$\dot{\tau}\frac{\partial \psi}{\partial \tau} = j\, p\omega_0\, \dot{\tau}\, g_p(\dot{\tau})\,\exp\, j(p\omega_0\tau + \omega_{//pc}t) \qquad (91)$$
$$\ddot{\tau}\frac{\partial \psi}{\partial \dot{\tau}} = \ddot{\tau}\frac{\partial g_0}{\partial \dot{\tau}} + \text{second order term} \frac{\partial g_p}{\partial \dot{\tau}} \ll \frac{\partial g_0}{\partial \dot{\tau}}$$

Limiting ourselves to first order terms, we obtain:

$$g_p(\dot{\tau}) = j\,\frac{\ddot{\tau}}{p\omega_0\dot{\tau} + \omega_{//pc}}\frac{\partial g_0}{\partial \dot{\tau}} \qquad (92)$$

in which

$$\ddot{\tau} = \frac{-\eta I Z_{//}(\Omega_c)}{(\frac{m_0c^2}{e})\gamma_0\beta_0^2}\,\exp\, j\left[p\omega_0\tau + \omega_{//pc}t\right]\int_{\dot{\tau}} g_p(\dot{\tau})d\dot{\tau} \qquad (93)$$

At first glance, it seems difficult to exploit this expression since the function g_p which gives the details of the initial perturbation appears explicitly. However, one can integrate both sides of the equation over $\dot{\tau}$ values. The equation then obtained from which the solution Ω_c will be drawn is called the Dispersion Relation. It is independent of g_p . In other words, the growth rate of the instability is independent of the exact form of g_p .

$$1 = \frac{\eta(\frac{q}{A})I}{(\frac{m_0c^2}{e})\gamma_0\beta_0^2}\; j\,\frac{Z_{//}(\Omega_c)}{p\omega_0}\int \frac{\frac{\partial g_0}{\partial \dot{\tau}}}{\frac{\omega_{//pc}}{p\omega_0} + \dot{\tau}}\, d\dot{\tau} \qquad (94)$$

The Dispersion Relation has been written for all types of particles :

$$\frac{q}{A} = 1 \text{ for protons or electrons}$$

$$q = \text{number of charges}$$

$$A = \text{number of masses}$$

$$\frac{m_0 c^2}{e} = \begin{matrix} \text{for heavy ions} \\ 0.511 \text{ MV for electrons} \\ 0.938 \text{ GV for protons} \\ 0.932 \text{ GV for heavy ions} \end{matrix} \tag{95}$$

A priori, the frequency shift $\omega_{//pc}$ appears twice,

$$1 = \frac{-\eta(\frac{q}{A})I}{(\frac{m_0 c^2}{e})\gamma_0 \beta_0^2} \; j \frac{Z_{//}(\Omega_c)}{p\omega_0} \int \frac{\frac{\partial g_0}{\partial \dot{\tau}}}{\frac{\omega_{//pc}}{p\omega_0} + \dot{\tau}} d\dot{\tau} \tag{96}$$

under the integral sign and as an argument of

$$Z_{//}(\Omega_c) = Z_{//}(p\omega_0 + \omega_{//pc}) \tag{97}$$

However, it is assumed that

$$\omega_{//pc} \ll p\omega_0 \tag{98}$$

and therefore, the value of the impedance can be taken at $p\omega_0$. Accordingly, we will write:

$$Z_{//}(\Omega_c) = Z_{//}(p) \tag{99}$$

We understand now why the quantity of interest is not

$$Z_{//}(p) \text{ but } \frac{Z_{//}(p)}{p} \tag{100}$$

To avoid carrying heavy expressions we will use the quantity:

$$\Lambda_{//} = \frac{\eta(\frac{q}{A})I}{2\pi\,(\frac{m_0c^2}{e})\gamma_0\beta_0^2} \tag{101}$$

and write the Dispersion Relation

$$1 = -\frac{2\pi}{\omega_0}\Lambda_{//}\, j\, \frac{Z_{//}(p)}{p} \int \frac{\frac{\partial g_0}{\partial \dot{\tau}}}{\frac{\omega_{//pc}}{p\omega_0} + \dot{\tau}}\, d\dot{\tau} \tag{102}$$

10. MONOCHROMATIC BEAM

We apply the Dispersion Relation

$$1 = -\frac{2\pi}{\omega_0}\Lambda_{//}\, j\, \frac{Z_{//}(p)}{p} \int \frac{\frac{\partial g_0}{\partial \dot{\tau}}}{\frac{\omega_{//pc}}{p\omega_0} + \dot{\tau}}\, d\dot{\tau} \tag{103}$$

to an infinitely cool beam with momentum $p_{//0}$:

$$g_0(\dot{\tau}) = \delta(\dot{\tau})$$

$$\int \frac{\frac{\partial g_0}{\partial \dot{\tau}}}{\frac{\omega_{//pc}}{p\omega_0} + \dot{\tau}}\, d\dot{\tau} = \frac{\omega_0}{2\pi}\left(\frac{\omega_{//pc}}{p\omega_0}\right)^{-2} \tag{104}$$

Finally one obtains:

$$\left(\frac{\omega_{//pc}}{p\omega_0}\right)^2 = -\frac{\Lambda_{//}}{\eta}\, j\eta\, \frac{Z_{//}(p)}{p} \quad \text{with} \quad \frac{\Lambda_{//}}{\eta}\ \text{positive} \tag{105}$$

1) Let us first consider a pure resistive component. The equation has two roots and whatever the sign of p, one of the two roots has $\mathrm{Im}(\omega_{//pc}) < 0$. The beam is unstable.

2) We assume now a pure space-charge interaction.

$$j\frac{Z_{// SC}(p)}{p} = \frac{Z_0 g}{2\beta_0\gamma_0^2} \text{ is real and positive} \qquad (106)$$

– below the transition energy ($\eta < 0$) the beam is stable.

– above the transition energy ($\eta > 0$) the beam is unstable (negative-mass instability).

3) We now consider the effect of a pure inductance, for instance the broad-band impedance at low frequencies. The results obtained with space charge must be inverted. In particular the beam is stable above transition.

The mathematical tools used to solve our problem (Vlasov's equation, Dispersion Relation, complex plane for frequencies and impedances, etc.) are very powerful. However, the physical meaning is rather lost in this series of mathematical treatments. We have begun with a prebunching of the beam with p wavelengths around the circumference. This prebunching coupled with the impedance creates a longitudinal force at a frequency close to $p\omega_0$ which reacts back on particles like an RF cavity would do. As a matter of fact the expression of $\omega_{//pc}$ is in all respects identical to the standard expression of the synchrotron frequency ω_S on a flat top of a magnetic field.

$$\omega_s^2 = \frac{-\eta(\frac{q}{A})\widehat{V_{RF}}\cos\phi_s\, h\omega_0^2}{2\pi\frac{m_0c^2}{e}\gamma_0\beta_0^2} \qquad \frac{\omega_{//pc}^2}{\omega_s^2} = \frac{[jZ_{//}(p)I]}{\widehat{V_{RF}}\cos\phi_s} \qquad (107)$$

$$\widehat{V_{RF}}\cos\phi_s \text{ is replaced by } [jZ_{//}(p)I] \qquad (108)$$

The results (curves corresponding to a given growth rate $\mathrm{Im}(\omega_{//pc})$), are generally represented in the impedance complex plane as shown below.

With the exception of the vertical axis (pure space charge below transition and broad band inductance above transition), all the working points in the impedance diagram correspond to an unstable motion. For a given impedance, the Dispersion Relation tells us at which rate a perturbation will grow. This is certainly the essential piece of information. However, the details of the evolution of the beam deterioration are inaccessible.

s.Let us qualitatively describe the instability in phase space. With a working point along the vertical axis in the unstable region (point A, Fig. 22), the resistive part of the impedance is null. The frequency shift $\omega_{//pc}$ has no real part which means that the RF field generated by the perturbation is exactly tuned to $p\omega_0$. The peaks of longitudinal density get trapped in the center of the buckets as shown in Fig. 23. The growth time is the synchrotron period in these bucket

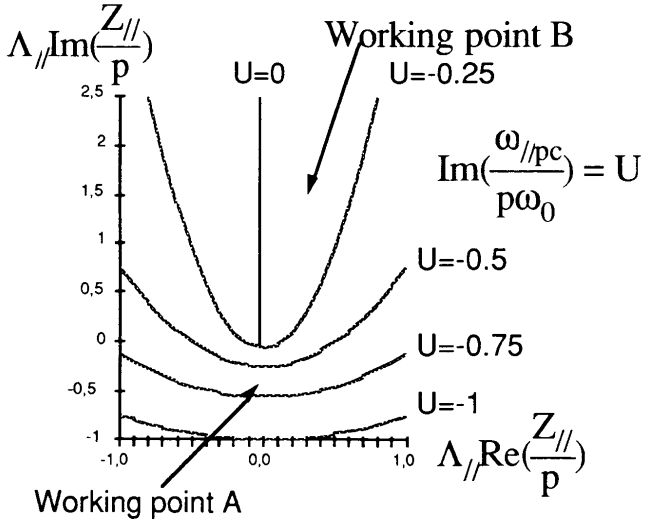

Fig. 22

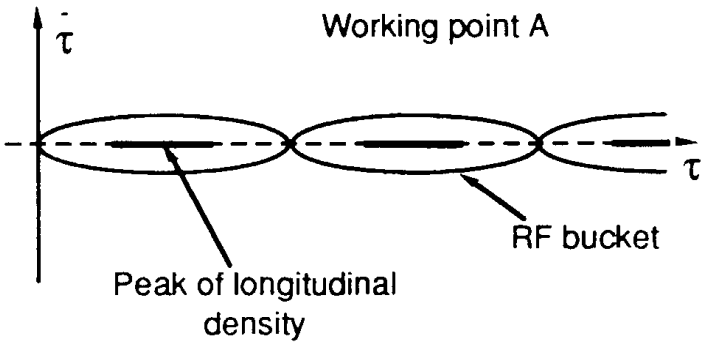

Fig. 23

When the working point is associated with a resistance (point B, Fig. 22), the frequency shift has both a real and an imaginary part. The RF buckets are generated at

$$\Omega_c = p\omega_0 + \mathrm{Re}\,(\omega_{//pc}) \tag{109}$$

The initially monochromatic beam starts wiggling far away from the bucket centers (Fig. 24).

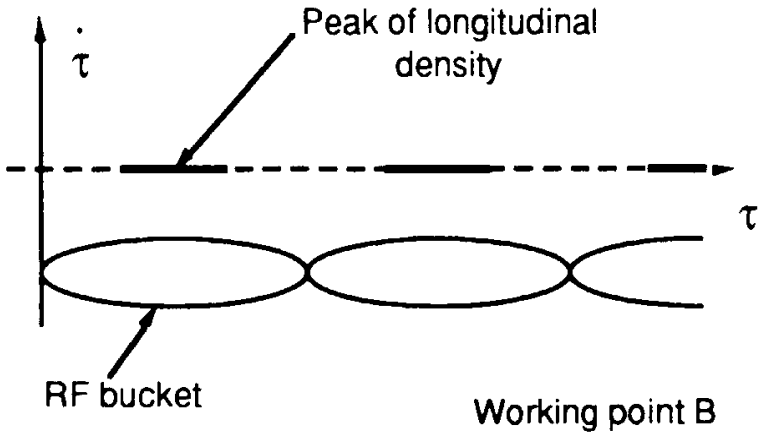

Fig. 24

As already indicated, the resistive part contributes directly to the imaginary part of the frequency shift.

$$\left(\frac{\omega_{//pc}}{p\omega_0}\right)^2 = - \; j\Lambda_{//} \frac{Z_{//}(p)}{p} \tag{110}$$

It is interesting to analyse the solution of the above equation by drawing the curves

$$\mathrm{Re}\left(\frac{Z_{//}(p)}{p}\right) \propto \frac{\mathrm{Im}(\omega_{//pc})}{p^2} \tag{111}$$

corresponding to a fixed growth rate in the frequency domain.

One can easily conclude that the resistive wall is far less harmful to the beam than the broad-band resistance peaked at high frequencies around the pipe cut-off frequency. In general the instability is of the microwave type with hundreds or thousands of mini-bunches around the circumference.

The conclusion of this section is that a cool beam with a very small momentum spread is unstable with respect to longitudinal instability. This is a problem to be faced by the new generation of cooler rings making use of either stochastic or electron cooling. There exists a threshold at which the instability growth rate is equal to the cooling rate. Under this threshold, the momentum spread can no longer be reduced.

The case of a beam with momentum spread is dealt with in the next section.

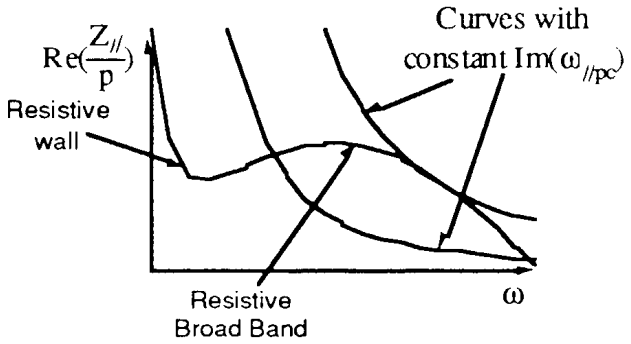

Fig. 25

11. COASTING BEAM WITH MOMENTUM SPREAD

It has been shown that in a ring, a very cool beam is subject to microwave instabilities which lead to a beam blow up in momentum. In this section, we will comment on the solution of the Dispersion Relation when a momentum spread is assumed. It will be shown that a sufficient momentum spread in the beam can cure the instability. Different realistic momentum distributions can be assumed. We will treat the case of a parabolic spread:

$$g_0(\dot{\tau}) = \frac{3\omega_0}{8\pi\dot{\tau}_L}\{1-(\frac{\dot{\tau}^2}{\dot{\tau}_L^2})\} \quad \text{for } |\dot{\tau}| \le \dot{\tau}_L$$
$$\text{and } \int_{\dot{\tau}} g_0(\dot{\tau})d\dot{\tau} = \frac{\omega_0}{2\pi} \text{ as required} \tag{112}$$

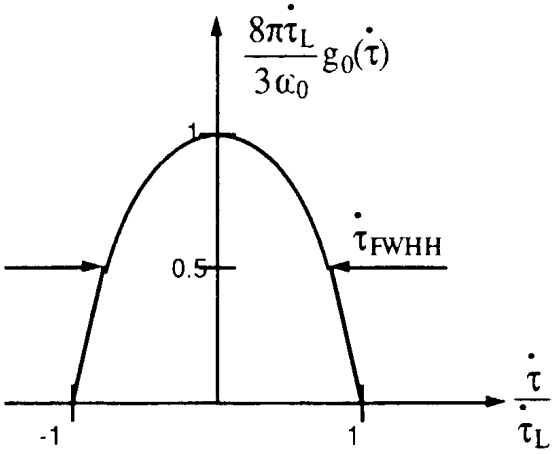

Fig. 26

The important quantity is the spread. Different distribution models with the same Full Width at Half Height spread behave almost identically. Only minor differences can be expected.

With the present model,

$$\dot{\tau}_{FWHH} = \sqrt{2}\dot{\tau}_L = \sqrt{2}|\eta|\left(\frac{dp}{p_{//}}\right)_L = |\eta|\left(\frac{dp}{p_{//}}\right)_{FWHH} \tag{113}$$

the Dispersion Relation can be split into real and imaginary parts:

$$\Lambda_{//C}\, Re(\frac{Z_{//}}{p}) = Im(J^{-1}) \text{ and } \Lambda_{//C}\, Im(\frac{Z_{//}}{p}) = -\, Re(J^{-1}) \tag{114}$$

by making use of the following notations:

$$\Lambda_{//c} = \frac{3\frac{q}{A}I}{2\pi\eta\frac{m_0c^2}{e}\gamma_0\beta_0^2\left(\frac{dp}{p_{//}}\right)^2_{FWHH}}$$

$$J = \int_{-1}^{+1} \frac{xdx}{x+\frac{\omega_{//}pc}{p\omega_0\dot{\tau}_L}} \tag{115}$$

In the stability diagram, the curves corresponding to a constant value of:

$$U = Im\left(\frac{\omega_{//}pc}{p\omega_0\dot{\tau}_L}\right) = Im\left(\frac{\sqrt{2}\omega_{//}pc}{p\omega_0|\eta|\left(\frac{dp}{p_{//}}\right)_{FWHH}}\right) \tag{116}$$

can be drawn.

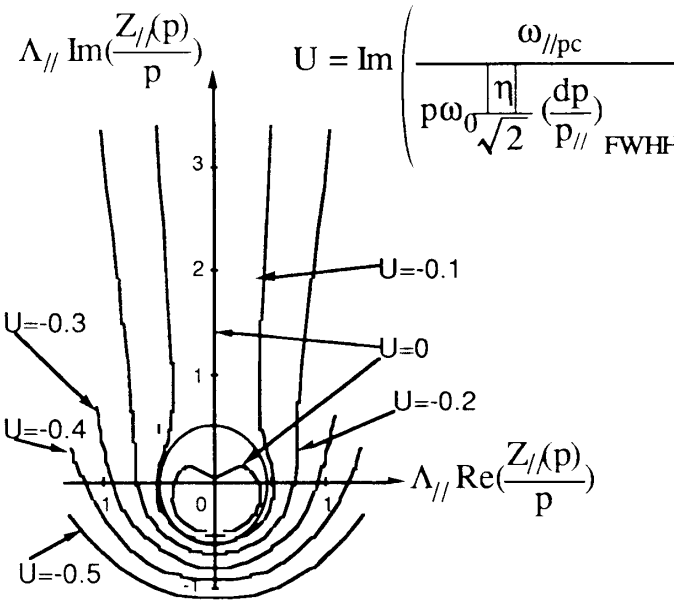

Fig. 27

The stability limit corresponds to the curve U = O. It is divided into two parts, the heart shape curve around the origin and the positive part of the vertical axis.

The actual shape of the stability limit depends on the distribution edges. Sharp edge distributions are less stable. A small rounding of the edges makes the contour more circular in the direction of the vertical axis. Distributions with long tails like a gaussian for instance are stable along the lower part of the vertical axis. When one neglects this distribution edge effect, the stability limit can be approximated by a circle.

$$\Lambda_{//c}\left|\frac{Z_{//}(p)}{\pi}\right| \le 0.5 \quad \text{or}$$
$$\left|\frac{Z_{//}(p)}{\pi}\right| \le \frac{m_0c^2}{e}\frac{\gamma_0\beta_0^2|\eta|}{\frac{q}{A}I}\left(\frac{dp}{p_{//}}\right)^2_{FWHH} \tag{117}$$

The minimum momentum spread required for stability is:

$$\left(\frac{dp}{p_{//}}\right)^2_{FWHH} \ge \frac{\frac{q}{A}I}{\frac{m_0c^2}{e}|\eta|\gamma_0\beta_0^2}\left|\frac{Z_{//}(p)}{p}\right| \tag{118}$$

12. LANDAU DAMPING BY MOMENTUM SPREAD

We can summarize the results of the last two sections as follows:

1) A monochromatic beam is unstable and the coherent frequency shift is given by:

$$\left(\frac{\omega_{//}pc}{p\omega_0}\right)^2 = \frac{-\eta\frac{q}{A}I}{2\pi\frac{m_0c^2}{e}\gamma_0\beta_0^2}\,j\,\frac{Z_{//}(p)}{p} \tag{119}$$

2) Stability requires a minimum spread in incoherent frequencies

$$\left(\frac{d\omega}{\omega_0}\right)^2_{FWHH} = \eta^2\left(\frac{dp}{p_{//}}\right)^2_{FWHH} \ge \frac{\frac{q}{A}I}{\frac{m_0c^2}{e}|\eta|\gamma_0\beta_0^2}\left|\frac{Z_{//}(p)}{p}\right| \tag{120}$$

It is clear that around the harmonic p of the revolution frequency the incoherent frequency band is pdω wide. The two formulae can be combined and the result can be expressed as follows: Stability requires the monochromatic beam coherent frequency shift to remain sufficiently inside the incoherent frequency band.

$$\left|\frac{\omega_{//}pc}{p\omega_0}\right| \le \sqrt{\frac{2}{\pi}}\left(\frac{d\omega}{\omega_0}\right)_{HWHH} = \sqrt{\frac{2}{\pi}}\left(\frac{pd\omega}{p\omega_0}\right)_{HWHH} \tag{121}$$

HWHH stands for Half Width at Half Height

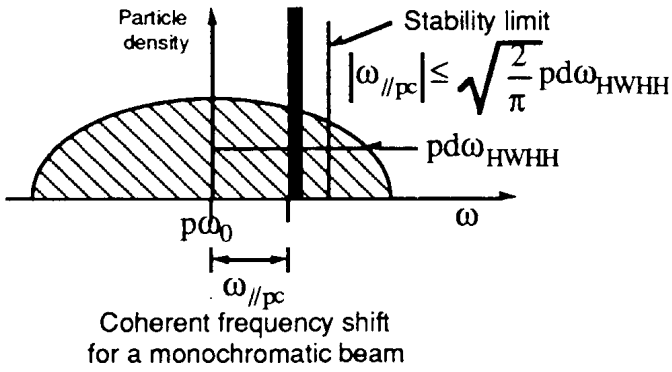

Fig. 28 Coherent frequency shift for a monochromatic beam

The stabilizing effect linked with the incoherent frequency spread is a general mechanism called Landau-Damping. The way it physically acts against the forces which drive the instability is hidden in Vlasov's equation which was used to establish the Dispersion Relation.

Let us try at least to qualitatively explain this Landau-Damping. We will proceed in two steps:

– We first ignore the self force and assume at t = 0 a prebunching of the beam with p wave lengths around the circumference.
  i) With a monochromatic beam, all particles have the same revolution frequency; the initial prebunching remains forever and a spectrum analyser indicates an infinitely narrow line at $p\omega_0$
  ii) Now, we introduce a spread in momentum and therefore in revolution frequency in the beam. The initial prebunching will disappear.

After a time interval

$$\Delta t = \frac{2\pi}{p d\omega_{FWHH}} \tag{122}$$

two particles which have a difference in revolution frequency equal to $d\omega_{FWHH}$ and which had started from the same position at t = 0 are now separated by one wavelength. Therefore, after Δt the prebunching has disappeared. Δt will be called the coherence time. Obviously, the larger the spread the shorter the coherence time.

After this introduction, we have all the elements to understand Landau-Damping. From now on, we reintroduce the self field. In the case of a monochromatic beam, the growth time of the instability is:

$$\tau_p = \frac{-1}{\mathrm{Im}(\omega_{//pc})} \tag{123}$$

There are two extreme cases.

In the first case, the incoherent frequency band is so narrow that the coherence time is much longer than the growth time of the monochromatic beam. Then, the beam behaves essentially like a monochromatic beam and blows up.

At the other extreme, the incoherent frequency band is so wide that the coherence time is much shorter than the monochromatic beam growth time. Then, the edges of the distribution

are rapidly out of phase with respect to the driving force. They do not contribute to the coherent signal anymore nor as a consequence to the amplitude of the force. The beam remains stable.

The regime where the beam is just at the stability limit stands between these two extreme cases. One can advance that the threshold is reached when the coherence time is of the order of the growth time.

$$- \mathrm{Im}(\omega_{//pc}) \approx p d\omega_{FWHH} \tag{124}$$

For comparison, in our summary of the results we noted:

$$|\omega_{//pc}| \leq \sqrt{\frac{2}{p}}\ p d\omega_{FWHH} \tag{125}$$

The order of magnitude is correct.

13. LIMITS OF THE THEORY

Several generations of accelerator physicists have worked on this problem of coherent instabilities. The synthesis of their work presented in the previous sections is a powerful and well established theory. This should not hide two major difficulties.

The first difficulty is that before applying this theory, one has to know the impedance of the ring perfectly. Unfortunately this is very difficult and even though a continuous effort is being made on the subject, the design of vacuum chambers is still largely empirical. Development of tools allowing for a more reliable approach to the design of vacuum chambers is progressing. A certain number of numerical codes solving Maxwell's equations in a structure excited by the passage of a mini bunch exist. They have been successfully tested on several types of structures. An example is shown for the Petra multicell RF cavities traversed by a short gaussian bunch.

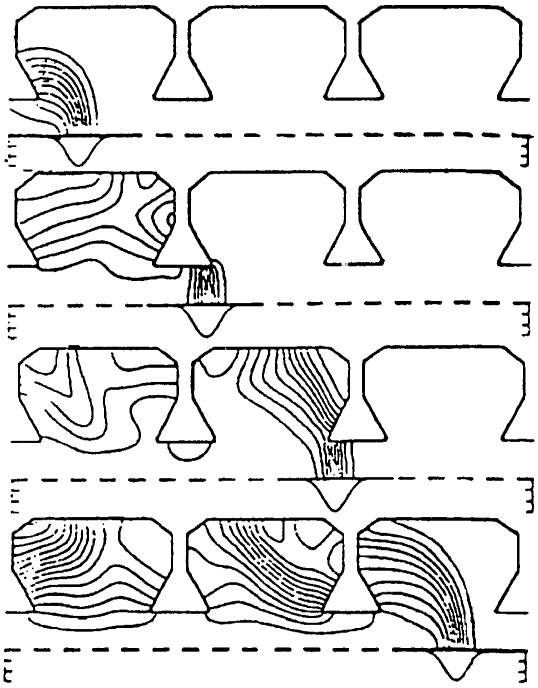

Fig. 29 Fields excited by a Gaussian bunch (σ = 2 cm) traversing a PETRA cavity

The second difficulty is that the theory has its own limitations. It is a perturbation theory which uses Vlasov's equation to first order. Therefore, it applies to conditions where the

instability remains very weak. Furthermore, the result drawn from this theory is a single complex number, namely the frequency shift. This is certainly an essential piece of information. However, in the case of unstable conditions, one cannot have access to the time evolution of the beam deterioration. To answer such a question, the only possibility is again to use numerical simulation codes working in the time domain.

An example of simulation is given in the next figure. It shows the development of a microwave instability. The beam-environment coupling assumes a broad band impedance centered around the pipe cut-off frequency. The simulation starts with an initial 10% longitudinal modulation of the particle density at the pipe cut-off frequency corresponding to harmonic 10 in the present case.

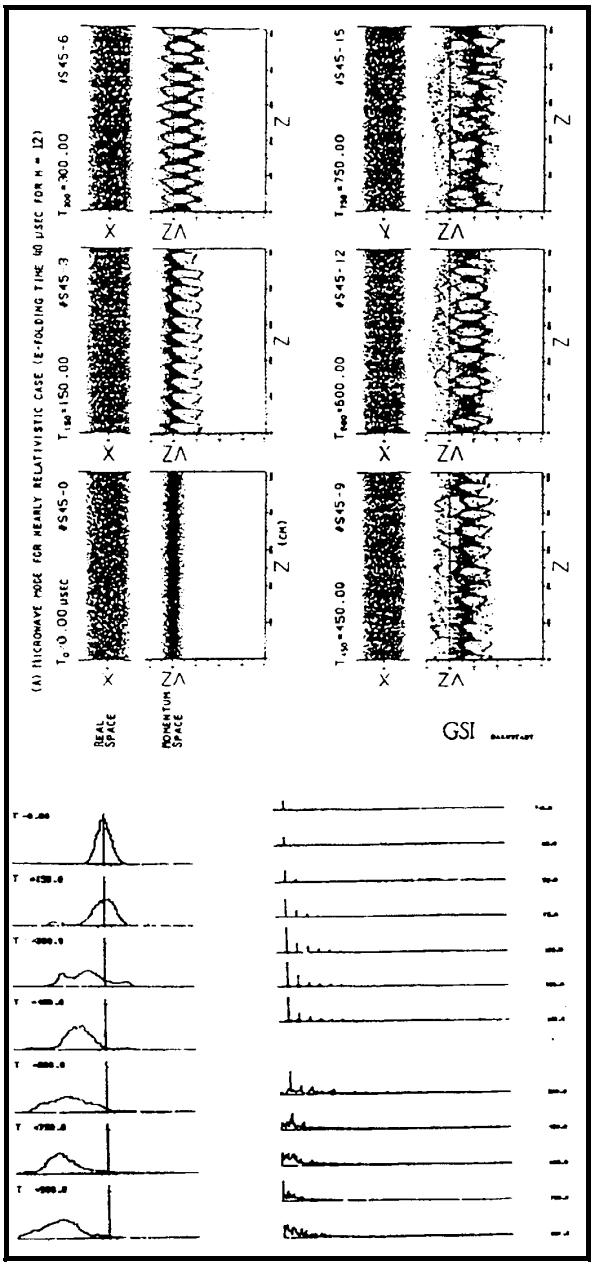

Evolution of Momentum Distribution Evolution of Fourier Spectra

Fig 30 Development of a longitudinal microwave instability

REFERENCES

[1] C.E. Nielsen et al., Proc. of Int. Conf. on High Energy Accel. and Instr., CERN (1959) 239

[2] V.K. Neil, R.J. Briggs, Plasma Physics, 9 (1967) 631

[3] V.K. Neil, A.M. Sessler, Rev. Sci. Instr. 36 (1965) 429

[4] B.W. Montague, Single Particle Dynamics, 3rd lecture, Int. School of Particle Accel., Erice (1976)

[5] B.W. Montague, Single Particle Dynamics, 5th and 6th lectures, Int. School of Particle Accel., Erice (1976)

[6] H.G. Hereward, Landau Damping, Int. School of Particle Accel., Erice (1976)

[7] K. Hübner, V.G. Vaccaro, CERN report ISR-TH/70-44 (1970)

[8] B. Zotter, CERN report ISR-GS/76-11 (1976)

[9] A.G. Ruggiero, V.G. Vaccaro, CERN report ISR-TH/68-33 (1968)

[10] E. Keil, W. Schnell, CERN report ISR-TH-RF/69-48 (1969)

[11] F. Sacherer, Proc. 1973 Part. Accel. Conf., San Francisco, IEEE Trans. Nucl. Sci. Vol. NS-20, n°3, 825

[12] F. Sacherer, CERN report SI/BR/72-5 (1972)

[13] A. Hofmann, Single beam collective phenomena-longitudinal, Int. School of Part. Accel., Erice (1976)

[14] I. Hofmann, Non linear aspects of Landau damping in computer simulation of the microwave instability, Computing in Accelerator Design and Operation, Berlin, Sept. 20-23 1983

[15] J.L. Laclare, Bunched-beam instabilities, 11th Int. conference on High Energy Accelerators, Geneva (July 1980) 526

[16] J.L. Laclare, Instabilities in storage rings, Proc. of the Symposium on Accelerator Aspects of H I Fusion, Darmstadt FRG (1982), GSI Report 82-8.